Available online at www.sciencedirect.com
ScienceDirect
Polymer 48 (2007) 4675–4682
polymer
www.elsevier.com/locate/polymer

Catalytic hydrolysis of *p*-nitrophenyl acetate by electrospun polyacrylamidoxime nanofibers

Liang Chen, Lev Bromberg, T. Alan Hatton*, Gregory C. Rutledge*

Department of Chemical Engineering, Massachusetts Institute of Technology, 77 Massachusetts Avenue, Cambridge, MA 02139, USA

Received 21 March 2007; received in revised form 31 May 2007; accepted 31 May 2007
Available online 9 June 2007

Abstract

Modification of polyacrylonitrile (PAN) by hydroxylamine resulted in polyacrylamidoxime (PANOx), the oxime groups of which are nucleophilic and capable of hydrolyzing esters. PANOx fiber mats with submicrometer fiber diameters ranging from tens to 300 nm were produced by electrospinning a suspension of PANOx blended with PAN (1:1 by weight) in a mixture of *N*,*N*-dimethyl formamide (DMF) and dimethyl sulfoxide (DMSO) (85:15 by weight). Catalytic properties of the PANOx nanofibers were tested by the hydrolysis of *p*-nitrophenyl acetate (PNPA), which mimics toxic organophosphate nerve agents and insecticides. The presence of PANOx fibers significantly accelerated the hydrolysis of PNPA compared to its spontaneous hydrolysis. The rate constants for the hydrolysis (k_1) and the deacetylation (k_2) reactions for the fibers were obtained using a proposed kinetic model. The effect of the fiber size on reaction rate indicated that intra-fiber diffusional resistances might limit the accessibility of the oxime catalytic sites in the fibers and affect their catalytic activity.

Keywords: Nanofiber; Catalysis; Nucleophile

1. Introduction

Military, fire fighting and medical personnel require a high level of protection when they face potential chemical or biological threats such as intentional or accidental release of chemical or biological agents. Chemical protective clothing systems in current use are essentially of the impermeable type, providing full barrier protection by physically or chemically adsorbing all the toxics on the surfaces of the fabrics [1]. Although they can offer sufficient protection, there are several disadvantages associated with such adsorptive protective clothing systems. Effective protection comes at the cost of wearing a bulky multilayer fabric system, which makes it heavy in weight and uncomfortable to wear due to the lack of breathability, i.e. low moisture vapor permeability. Furthermore, contamination by secondary vapors may arise as the adsorbed toxic chemicals subsequently desorb from the surfaces of the fabrics. This motivates the development of a new generation of chemical protective garments that are lightweight and can detoxify the toxic chemical agents on fabrics or selectively block toxic chemicals while maintaining fabric breathability.

Electrospinning technology has attracted growing scientific interest due to the affordability of this process and the unique properties of electrospun fiber meshes [2–5]. In electrospinning processes electrostatic forces are applied to stretch a polymer jet and produce continuous fibers with diameters ranging from micrometers to nanometers [6–12]. Electrospun nanofibers possess high specific surface area, high porosity, small fiber diameter and low weight. These unique properties have triggered a broad range of applications, including composite materials [13,14], sensors [15], scaffolds in tissue engineering [16], nanodevices [17], and filtration [18,19]. Electrospinning also offers a practical means to produce high surface area, microporous nanofiber mats, which can serve as carriers of

* Corresponding authors.
E-mail addresses: tahatton@mit.edu (T.A. Hatton), rutledge@mit.edu (G.C. Rutledge).

0032-3861/$ - see front matter © 2007 Elsevier Ltd. All rights reserved.
doi:10.1016/j.polymer.2007.05.084

reactive compounds or functional groups capable of destroying toxic chemicals, and which can be used in the development of self-detoxifying protective clothing. For example, Schreuder-Gibson et al. reported that electrospun polyurethane fibers containing matrix-bound polyoxometalates (POMs) catalytically decontaminated mustard simulants [20].

In this work, we report on catalytic, electrospun, nonwoven nanofiber mats composed of polyacrylamidoxime (PANOx) blended with polyacrylonitrile (PAN), which potentially can be incorporated into self-detoxifying protective clothing as reactive or catalytic layer(s). The oxime groups or oximate ions are among the most powerful α-nucleophiles because of the electronic repulsion between the lone electron pairs on the nucleophilic oxygen atom and the adjacent nitrogen atom, which can be reduced and can consequently stabilize the transition state upon nucleophilic attack onto a substrate. Therefore, oximes are capable of nucleophilic hydrolysis of ester groups. It is known that oximate ions are 100-fold more reactive than phenolate ions of the same pK_a [21]. Oximes have been widely used as reactivators of acetylcholinesterase inhibited by organophosphate pesticides or nerve agents, i.e., as antidotes [22]. Colloidal oximes in the form of micelles and particles have been studied in connection with the decomposition of organophosphates or nitrophenyl acetate [21,23–28], and it has been shown that the hydrolysis of phosphate esters or analogous substrates is catalyzed efficiently by oximate ions or oximes. In this work, we have selected *p*-nitrophenyl acetate (PNPA) as a model compound for the more toxic organophosphates or chemical nerve agents, and have studied the catalytic properties of PANOx/PAN electrospun nanofibers on the hydrolysis of this substrate. Hydrolytic pathways of the PNPA esterolysis have been widely used to elucidate nucleophilic decomposition of more toxic organophosphates [29,30].

2. Experimental method

2.1. Materials

Polyacrylonitrile (PAN) (M_w 150 kDa) was purchased from Polysciences Inc. (Warrington, PA) and used as received. *N*,*N*-Dimethyl formamide (DMF), dimethyl sulfoxide (DMSO), hydroxylamine hydrochloride and *p*-nitrophenyl acetate (PNPA) were purchased from Sigma–Aldrich Chemical Co. (St. Louis, MO) and used as received.

2.2. Reactive polymer preparation

Polyacrylonitrile (PAN) was modified to obtain catalytic polyacrylamidoxime (PANOx) by conversion of acrylonitrile groups to acrylamidoximes via reaction of PAN with excess hydroxylamine hydrochloride in methanol or DMF at 80 °C under reflux for 24 h, as shown in Scheme 1. The resulting polymers were repeatedly washed with methanol, acetone and water followed by drying under vacuum until constant weight. Fig. 1 shows FTIR spectra of the unmodified PAN and of the PANOx product. Complete conversion of acrylonitrile groups of PAN to the amidoxime groups was confirmed

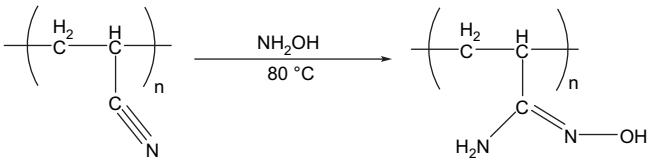

Scheme 1. Modification of polyacrylonitrile to polyacrylamidoxime.

by observing the disappearance of the original nitrile groups of PAN at 2260 cm^{-1} (stretching vibration of nitrile group) and appearance of the acrylamidoxime groups (stretching vibration of C=N at 1670 cm^{-1}, scissor vibration of NH_2 at 1610 cm^{-1} and stretching vibration of NH_2 and OH at 3100–3600 cm^{-1}).

2.3. Electrospinning

The well-documented formation of the glutaroimide–dioxime links between PANOx segments (Scheme 2) limits the solubility of PANOx in common organic solvents [31].

In our experiments, the PANOx did not dissolve in DMF but was observed to form clear solutions in DMSO at polymer concentrations not exceeding 2 wt%. At larger PANOx concentrations in DMSO, some turbidity ensued. On the other hand, DMF appeared to be a good solvent for PAN and was observed to facilitate the electrospinning process. Therefore, a DMF/DMSO solvent mixture that afforded stable suspensions of partially dissolved PANOx in viscous PAN solutions was used in this work. The unmodified PAN was blended with PANOx to increase the total polymer concentration in order to provide sufficient elasticity of the solution or dispersion for successful electrospinning. A homogenized 6–8 wt% PANOx/PAN (1:1 by weight) blend was prepared by dissolution in DMF/DMSO (85:15 w/w) under vigorous stirring for several days at room temperature.

A parallel plate electrospinning setup previously described by Shin et al. [32] was used. Two aluminum disks 15 cm in diameter were arranged parallely at 20–30 cm apart. The polymer suspension was delivered to a capillary nozzle via a Teflon feedline from a syringe pump (Harvard Apparatus PHD 2000, Holliston, MA). Three sizes of nozzles were used: 1.02 mm (0.04″), 0.76 mm (0.03″) and 0.51 mm (0.02″) inner diameter. Most nanofibers used in this study were electrospun from the nozzle of 1.02 mm in diameter. The other two nozzles were used for producing nanofibers of various size to study the effect of fiber size on the fiber performance. The spinneret protruded through the center of the upper plate to a length of 2 cm. A power supply (Gamma High Voltage Research ES-30P, Ormond Beach, FL) provided up to 30 kV to the upper disk. In some cases, a rotating drum ground electrode was used to collect the electrospun nanofibers since the nanofibers were charged and difficult to collect on a plate collector. The applied electrical potential (25–30 kV), the solution flow rate (0.005 ml/min) and the distance between the capillary tip and the collector (20–30 cm) were adjusted to obtain a stable jet.

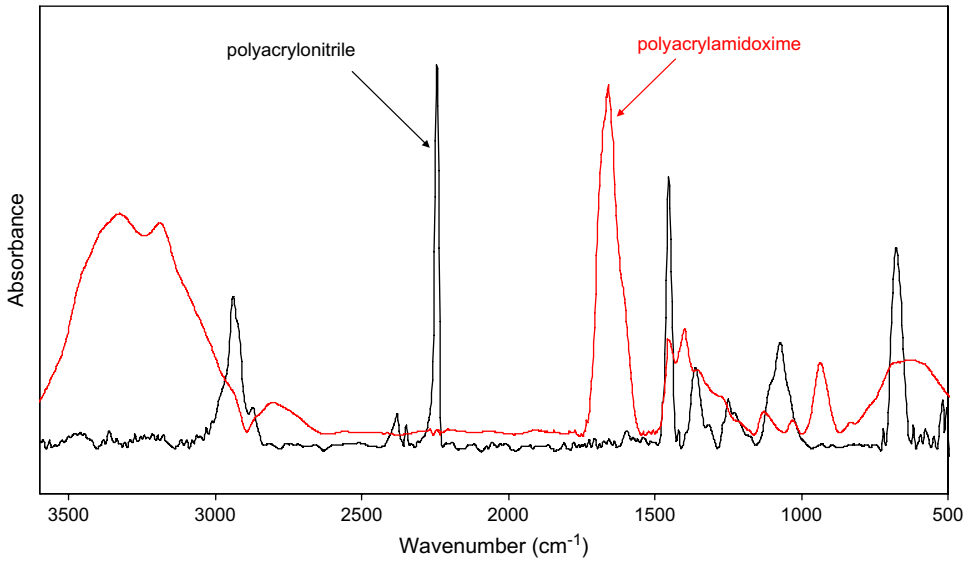

Fig. 1. FTIR spectra of untreated PAN and PANOx that resulted from the treatment of PAN with hydroxylamine.

2.4. Characterization

Morphology of the electrospun fibers was visualized by scanning electron microscopy (SEM, JEOL-6060). A thin layer of gold was sputter-coated onto the nanofibers to avoid charging problems. Fiber diameters were determined using AnalySIS image processing software (Soft Imaging System Corp., Lakewood, CO).

Fourier transform infrared spectra (FTIR) were measured using a Nexus 870 spectrophotometer (Thermo Nicolet Corp., Madison, WI) in absorbance mode by accumulation of 256 scans with a resolution of 4 cm^{-1}.

BET surface areas of electrospun nanofibers were determined with an ASAP 2020 accelerated surface area and porosimetry analyzer (Micromeritics Instrument Co., Norcross, GA).

Kratos Axis Ultra Imaging X-ray photoelectron spectrometer (XPS) (Kratos Analytical Co., Chestnut Ridge, NY) was used to measure the surface compositions of nanofibers with a monochromatized Al Kα X-ray source.

2.5. Kinetics

Hydrolysis kinetics were measured using a Hewlett Packard 8453 UV–Vis spectrophotometer equipped with a thermostated cell compartment. The time progression of the reaction of PNPA with the nanofibers was followed by measuring the appearance of the *p*-nitrophenolate ions at 405 nm. Because of the negligible solubility of the PNPA in water as well as limited wettability of the PANOx/PAN nanofiber surface by water, a mixture of 50 mM Tris buffer and ethanol was applied as a reaction milieu. In a typical experiment, 1 ml of freshly made PNPA/ethanol solution was added into a suspension of a weighed amount of the electrospun nanofibers in 9 ml of stirred 50 mM Tris buffer/ethanol (1:1 by volume) solution. The pH value of the reaction medium was adjusted before the commencement of the reaction and measured after the reaction by a digital pH meter to assure that the pH did not change during the course of the reaction. The temperature was maintained at 25 °C.

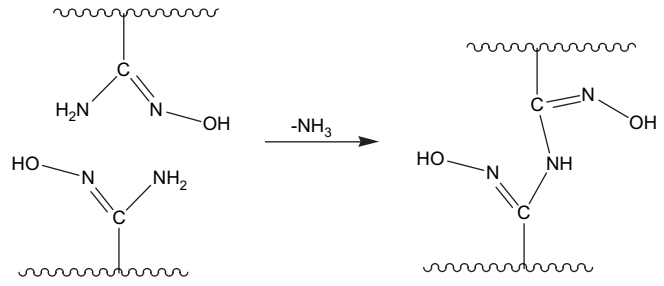

Scheme 2. Formation of glutaroimide–dioxime bonds between polyacrylamidoxime chains.

3. Results and discussion

Fig. 2 shows a typical SEM image of the electrospun PANOx/PAN nanofibers produced in this work. The average diameter of these nanofibers was about 170 nm with the fiber diameters ranging from 100 to 300 nm. The measured BET surface area of these nanofibers was about 14.8 m^2/g. Characteristic peaks of the nitrile groups (2260 cm^{-1}) and amidoximes (1670 cm^{-1}, 1610 cm^{-1} and 3100–3600 cm^{-1}) were observed in the FTIR spectra of PAN/PANOx nanofibers, which confirmed the presence of both PAN and PANOx in the nanofibers. Furthermore, elemental analysis showed that the initial ratio of the PAN to PANOx (1:1 by weight) set in the electrospun dispersion was maintained in the fibers.

The mechanism of esterolytic cleavage of PNPA by nucleophiles in homogeneous solutions has been investigated in some detail [33–36]. The novelty of this work stems from the fact that the hydrolysis occurs in a heterogeneous system with catalytic nanofibers that are insoluble in the aqueous/ethanol medium in which the substrate PNPA is dissolved. The pathway of the PNPA nucleophilic hydrolysis in aqueous

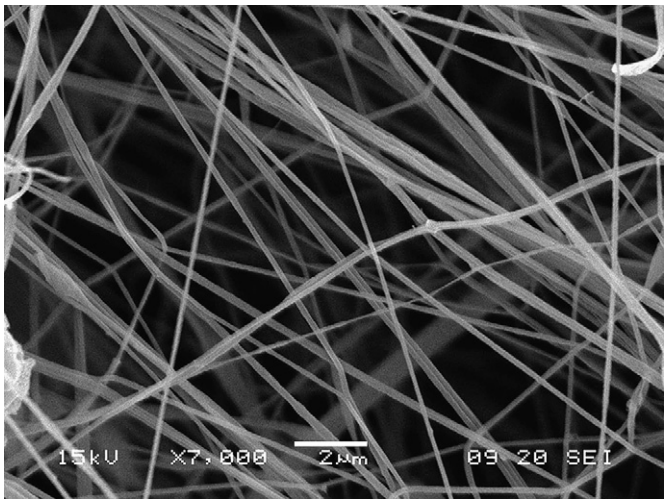

Fig. 2. A typical SEM image of electrospun PANOx/PAN nanofibers (average fiber diameter: 170 ± 40 nm, scale bar: 2 μm).

media is well established [37,38]. Scheme 3 shows a schematic diagram of the PNPA hydrolysis catalyzed by the electrospun PANOx/PAN nanofibers. The PNPA substrate (S) is attacked by the catalytic acrylamidoxime group (C), which results in a polymer with acetylated acrylamidoxime groups (CS) and a product (P_1) comprising a mixture of nitrophenol and nitrophenolate ions. The precise composition of the product P_1 depends on the pH of the reaction medium, with the *p*-nitrophenol possessing a pK_a of 7.2 [39]. Water facilitates the deacetylation of the transition compound (CS) and regeneration of the catalytic oxime groups (C), releasing the acetate product (P_2) into the medium.

Fig. 3 shows typical kinetics of the PNPA esterolytic hydrolysis in the presence of the PANOx/PAN nanofiber as well as spontaneous hydrolysis at various pHs. The catalytic reactions were carried out under conditions of excess catalytic oxime groups relative to the initial substrate concentration, i.e., $[Ox]_a > [PNPA]_o$, where the apparent oxime concentration, $[Ox]_a$, was defined based on the volume of the reaction solution. As shown in Fig. 3(a), hydrolysis in the presence of the fibers proceeded via an initial rapid formation of product P_1 followed by a slower steady process. The initial reaction rates were calculated from the initial slopes of the conversion *vs*. time curves:

$$r = \frac{\Delta \text{Conversion}}{\Delta t}[\text{PNPA}]_o \quad (1)$$

In the case of the fiber-aided hydrolysis, the observed reaction rate consisted of the catalytic and spontaneous terms:

$$r = r_{cat} + r_{sp} \quad (2)$$

The rates of these hydrolysis reactions increased with increasing pH, the catalytic hydrolysis rate being 3–7-fold faster than the spontaneous hydrolysis rate at all pHs studied in the case of $[Ox]_a$ of 2.91 mM. In a control experiment, the hydrolysis of PNPA in the presence of the non-catalytic PAN nanofibers under identical conditions was observed to be identical to that of the spontaneous hydrolysis of PNPA in the absence of nanofibers, which further confirmed the catalytic activity of the PANOx/PAN nanofibers.

Fig. 4 shows two independent series of experiments in which the initial catalytic reaction rates, r_{cat}, were measured with (a) varying PNPA initial concentrations at fixed fiber apparent concentration; and (b) varying fiber content in the reaction medium at fixed initial substrate concentration. The r_{cat} is obtained by subtraction of the independently determined rate of the spontaneous hydrolysis (r_{sp}) from the experimentally measured initial reaction rate (r), according to Eq. (2). As shown in Fig. 4(a), the initial reaction rate increased and gradually reached a plateau as the substrate concentration increased. We attribute this to full occupation of all the oxime catalytic sites by the substrate molecules when the concentration of PNPA exceeds the catalytic oxime concentration. Fig. 4(b) shows that the reaction rate is proportional to the fiber content in the reaction mixture if $[PNPA]_o$ is kept constant. At $[Ox]_a = 8$ mM, the catalytic reaction rate is 20-fold faster than that of the spontaneous hydrolysis.

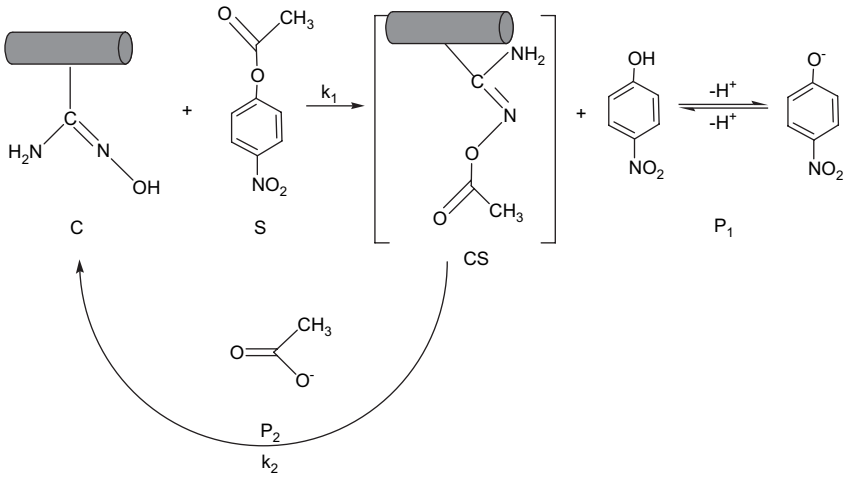

Scheme 3. Catalytic hydrolysis of PNPA by acrylamidoxime groups on the nanofibers.

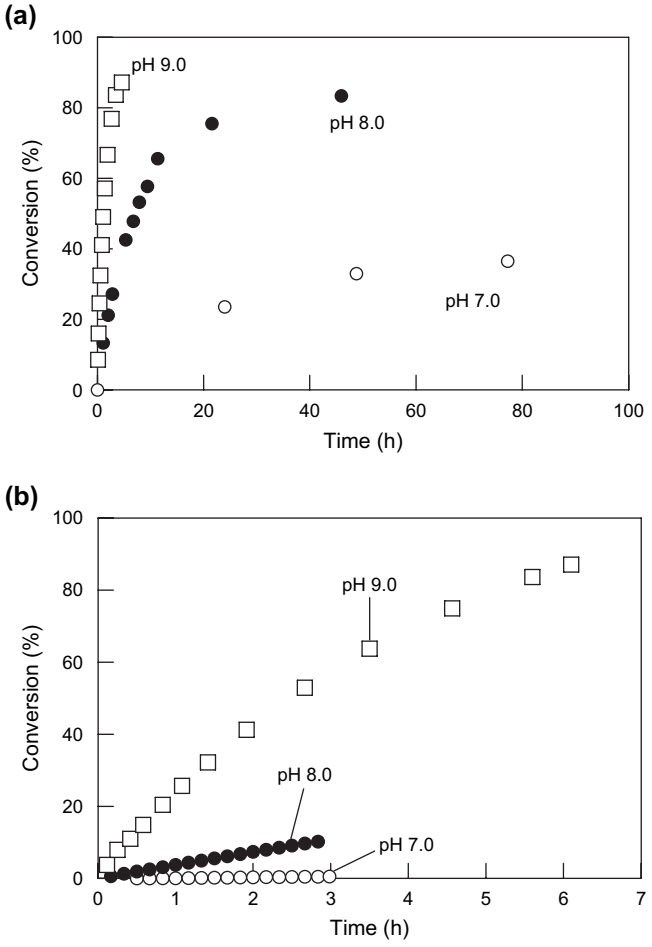

Fig. 3. Kinetics of PNPA conversion with (a) and without (b) nanofibers presented as functions of pH. $[Ox]_a = 2.91$ mM, $[PNPA]_o = 5.52 \times 10^{-5}$ M.

According to Scheme 3, the rate of steady-state hydrolysis can be expressed as [38]:

$$r_{cat} = \frac{d[P_1]}{dt} = \frac{k_1 k_2 [C]_o [S]}{k_1 [S] + k_2} \quad (3)$$

where $[P_1]$, $[C]_o$ and $[S]$ are the product P_1 concentration, total catalyst concentration, and substrate concentration, respectively (for designations, see Scheme 3). Eq. (3) allows for estimation of the rate constants of the hydrolysis (k_1) and deacetylation (k_2) reactions based on the experimental measurement of accumulation of the product, P_1. Linear fits in the initial catalytic reaction rate *vs.* $[Ox]_a$ plot for constant $[PNPA]_o$ and reciprocal initial catalytic reaction rate *vs.* reciprocal substrate concentration for constant $[Ox]_a$ were obtained with $R^2 > 0.99$, and are shown in Fig. 4(b) and (c). These results, along with the measurements of the rate of spontaneous hydrolysis, enabled estimation of both k_1 and k_2, which are given in Table 1. Both the spontaneous hydrolysis rate constant (k_{sp}) as well as k_1 increase as the pH changes from 7.0 to 8.0, since the pH affects the basicity, $[OH^-]$, of the solution and the weight ratio of more reactive oximate ions to the neutral oxime groups in the fibers, while the deacetylation constant, k_2, shows only a weak pH-dependence. The relatively low deacetylation rate, which is comparable to that of the spontaneous hydrolysis at pH = 8.0, is responsible for a low rate of recovery of the catalytic sites, and hence a reduction in the overall rates of reaction as the reaction proceeds.

With heterogeneous catalysis in the presence of fibers, a significant reduction in the PNPA hydrolysis rate was observed after a short, initial rapid stage, resulting in lower product conversions at pH 7.0 and 8.0 than if the rates had remained unchanged (Fig. 3(a)). This effect was associated with the low catalyst turnover rate, which was limited by the rate of deacetylation, k_2. It has been shown that, even in the process of homogeneous catalysis with water-soluble polymers, the rate of deacetylation of the catalytic oxime sites significantly limited the catalyst turnover rate [37]. We believe that mass transfer phenomena and the desorption of the acetate ion from the fiber could slow the deacetylation even further, effectively blocking the catalytic sites and limiting the overall hydrolysis rate at its later stage. In addition, the electrospun nanofibers with their high specific surface area could adsorb and retain undissociated nitrophenol and acetates efficiently, effectively inhibiting the catalytic activity of these sites when the nitrophenol concentration reaches a certain level after the initial stages of the hydrolysis, especially at pH 7.0. The retention of nitrophenol and acetate and relatively slow catalyst turnover rate were confirmed by the FTIR spectra of the nanofibers after reaction, which were recovered, washed and dried before the measurement. After completion of the reaction, the fibers exhibited a significant degree of acetylation as evidenced by the strong band of carbonyl groups (>C=O stretch) in the area of 1700 cm^{-1} and 1760 cm^{-1}.

The narrow operational window for successful electrospinning with respect to the flow rate and the concentration of the solution/suspension did not readily permit manipulation of the size of the electrospun PANOx/PAN nanofibers over a wide range. Therefore, some control of the fiber sizes was achieved by the use of the capillary nozzles of various sizes. As shown in Table 2, the average nanofiber diameter was reduced from 170 to 90 nm when the smaller nozzle size, 0.76 mm inner diameter, was employed. Further reduction in the capillary nozzle size did not lead to obvious changes in nanofiber size. Previous work has shown that there exists a terminal jet diameter that arises from an asymptotic force balance between surface tension and surface charge repulsion [12]. We speculate that this terminal jet diameter may have been reached, thus preventing further thinning of the polymer jets. The nanofiber BET surface area, which is inversely proportional to the fiber diameter, almost doubled from 14.8 to 26.6 m^2/g as the fiber size reduced by half. Experimental results indicated that the catalytic reaction rates under identical reaction conditions increased by 60% as the surface area of the fibers increased by 80%. It has been reported that the mass transfer, intraparticle diffusion, and catalyst structure affect the reactivity of insoluble heterogeneous polymer-supported catalyst particles with the size ranging from tens to 300 nm [40]. In this work, vigorous mechanical stirring was carried out to eliminate resistances to the diffusional transport of the substrate from the

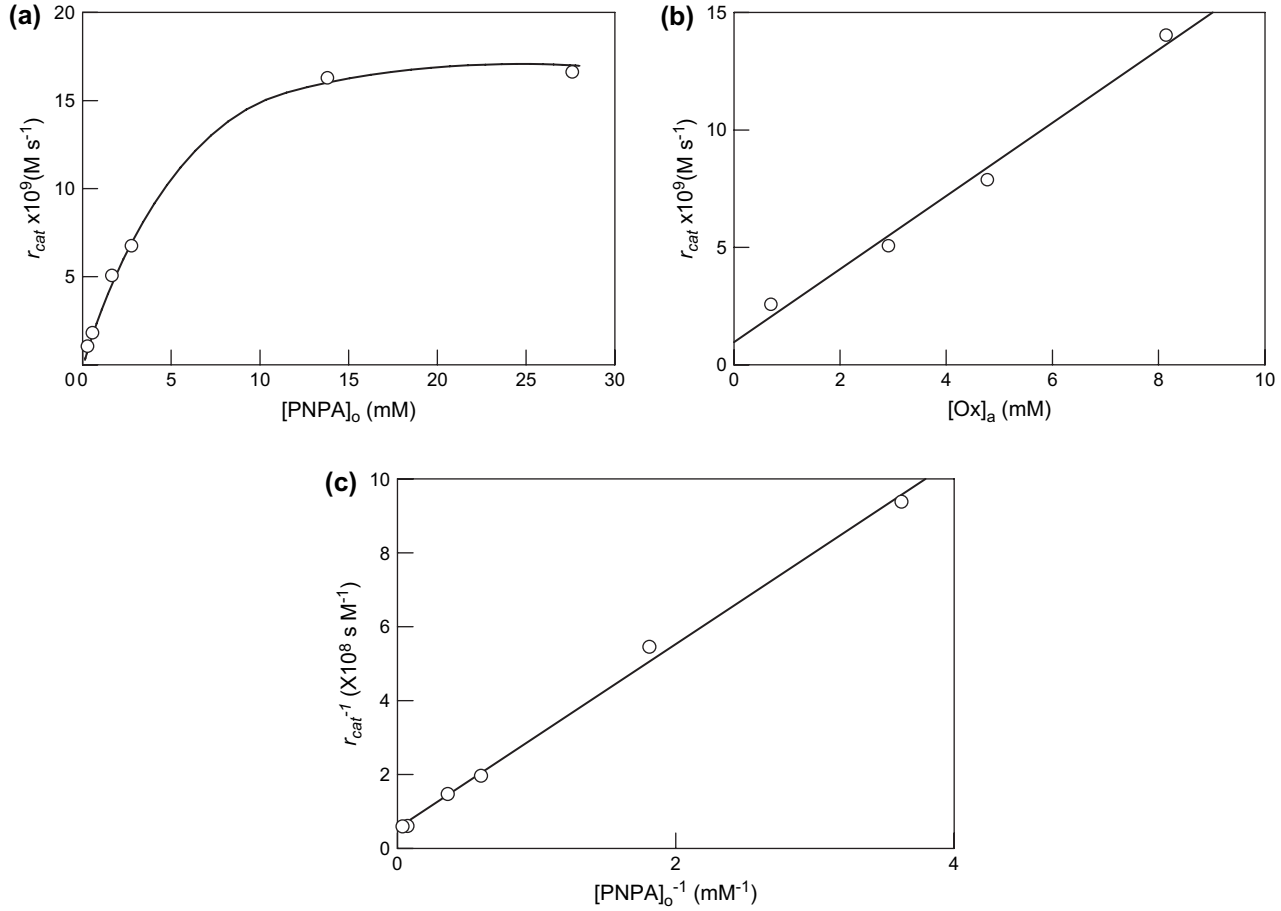

Fig. 4. Observed catalytic reaction rate (r_{cat}) as a function of the initial substrate concentration ([PNPA]$_o$) and apparent concentration of the oxime groups in the fibers ([Ox]$_a$) for pH = 7.0. (a) [Ox]a = 2.91 mM; (b) [PNPA]$_o$ = 1.66 mM; (c) [Ox]$_a$ = 2.91 mM.

bulk liquid to the catalyst surface [40]. The intra-fiber diffusion of the substrate to the active catalyst sites buried within the fibers and of the product to the external solution could significantly affect the availability of the catalyst sites in the fibers. A smaller fiber with larger surface area ensured that a greater fraction of the oxime functional groups would be located on or close to the surface of the nanofibers, and would thus be exposed to and attacked by the substrate in the solution more readily. The fibers with the smaller diameter also offer shorter diffusional paths to the active catalyst sites in the fiber cores. XPS data shown in Fig. 5 revealed that the surface layer within 6 nm of the fiber surface consists of an atomic ratio of 16:1 of carbon to oxygen for the fibers of 170 nm diameter, which is twice the atomic ratio of 8:1 in the bulk material composition. This result is indicative of the presence of more oxime groups in the bulk of the fibers than on their surfaces. We speculate that bonding between segments of the PANOx macromolecule tends to lead to the oxime groups being confined within the nanofibers rather than reporting to their surfaces. Although the addition of PAN facilitated the electrospinning of the PANOx, it also limited the surface concentration of the oxime groups and influenced the accessibility of the catalyst sites. We believe that the diffusional limitations of the substrate to the majority of oxime catalytic sites within the nanofiber cores significantly limited the availability of the catalyst sites in the fibers and affected the reactivity of the fiber catalysts. Our estimate of active oxime groups based on the initial oxime concentration [Ox]$_a$ ignored the diffusion

Table 1
Kinetics constants of PNPA catalytic hydrolysis (k_1), product deacetylation (k_2) and spontaneous hydrolysis (k_{sp})

pH	$k_1 \times 10^3$ (M^{-1} s^{-1})	$k_2 \times 10^6$ (s^{-1})	$k_{sp} \times 10^6$ (s^{-1})
7.0	1.38	4.86	0.648
8.0	7.91	5.20	9.49
9.0	–[a]	–[a]	64.4

[a] Parameters could not be accurately determined.

Table 2
Fiber size effect

Nozzle size (mm)	Average fiber size (nm)	BET surface area (m^2/g)	$r \times 10^9$ (M/s)[a]
1.02	170 ± 40	14.8 ± 0.1	6.7 ± 0.7
0.76	90 ± 30	26.6 ± 0.2	10.5 ± 1.6
0.51	80 ± 30	25.9 ± 0.1	9.9 ± 0.8

[a] The initial reaction rates (r), defined in Eq. (1), were measured at pH = 8.0, 25 °C, [Ox]$_a$ = 2.91 mM and [PNPA]$_o$ = 2.76 × 10^{-4} M.

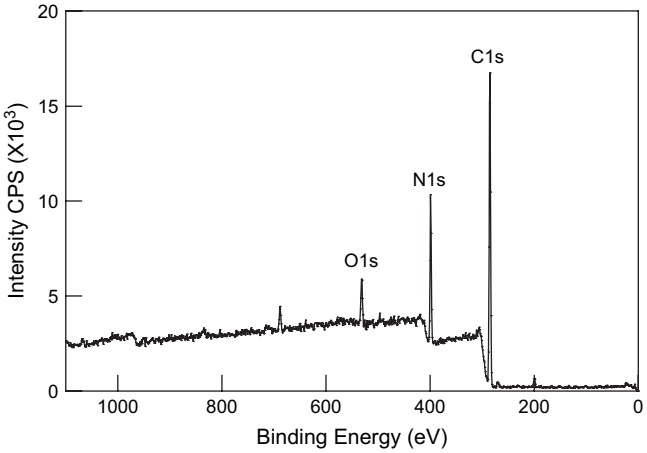

Fig. 5. XPS spectrum of the electrospun nanofibers of the PANOx/PAN blend.

inside the fibers, over-counted the accessibility of all the oxime groups in the fibers and underestimated the hydrolysis constant (k_1). This could explain the order of magnitude slower hydrolysis constant (k_1) of the PANOx/PAN nanofibers obtained in this work, compared to that in the homogeneous reaction catalyzed by a water-soluble copolymer of phenylisobutyrohydroxamic acid and 1-vinyl-2-methylimidazole in aqueous medium [37]. On the other hand, it is known that the hydrolysis of PNPA is significantly influenced by the solvent used [33,41]. The esterolysis of PNPA in ethanol is approximately 100-fold slower than that in water, which contributed to the lower k_1 as well. We surmise that significant improvements in the fiber catalyst reactivity will result from either further reduction of the fiber diameter (minimizing the effect of the intra-fiber diffusion) or immobilization of the majority of the catalytic sites on the fibers surface, which will eliminate the limitation of the intra-fiber diffusion.

4. Concluding remarks

Functionalized oxime nanofibers were produced via electrospinning of a dispersion of PANOx blended with PAN. The functioning of this fiber-based heterogeneous catalyst was tested in the hydrolysis of PNPA, a model compound for the more toxic organophosphates and nerve agents. The release of nitrophenolate, as monitored by UV–Vis measurements, revealed that the presence of the PANOx nanofibers remarkably accelerated the hydrolysis of PNPA in aqueous/ethanol solutions at pH ranging from 7.0 to 9.0. The dependence of the reaction rate on the fiber size indicated that intra-fiber diffusional limitations might affect the accessibility of oxime catalytic sites inside the fibers significantly, and that the catalytic hydrolysis probably occurs primarily on the surface of the oxime nanofibers. This work demonstrates the concept of incorporation of the α-nucleophilies into the electrospun nanofibers capable of catalytically decomposing toxic chemicals. Previously, attachment of functionalized nanoparticles to fibers and textiles has been described that imparted bioactive, fragrant, insect repellent, etc. properties to the fiber surfaces [42]. In contrast to the present work, the chemistry of the particle grafting onto the fibers did not permit to maintain the reactivity of the oxime and other nucleophilic functionalities incorporated into the fibers [42]. However, in light of possible diffusional limitations observed herein, we plan on adopting a somewhat analogous concept of having the majority of the reactive groups on the fiber surface. Allocating all of the active catalytic sites on the fiber surface rather than distribution of the catalyst in the whole volume of the fibers should improve the catalyst reactivity. We envision utilization of such self-detoxifying, lightweight nanofibers as key functional layers in a new generation of protective fabrics and filters.

Acknowledgments

This research was supported by the DuPont-MIT Alliance (DMA). The authors thank the Institute for Soldier Nanotechnologies (ISN) and the Center for Materials Science and Engineering (CMSE) at MIT for use of their facilities.

References

[1] Schreuder-Gibson HL, Truong Q, Walker JE, Owens JR, Wander JD, Jones WE. MRS Bull 2003;28:574.
[2] Dzenis Y. Science 2004;304:1917.
[3] Li D, Xia Y. Adv Mater 2004;16:1151.
[4] Ramakrishna S, Fujihara K, Teo W-E, Lim T-C, Ma Z. An introduction to electrospinning and nanofibers. Singapore: World Scientific Publishing Company; 2005.
[5] Huang Z-M, Zhang Y-Z, Kotaki M, Ramakrishna S. Compos Sci Technol 2003;63:2223.
[6] Reneker DH, Yarin AL, Fong H, Koombhongse S. J Appl Phys 2000;87:4531.
[7] Yarin AL, Koombhongse S, Reneker DH. J Appl Phys 2001;89:3018.
[8] Yarin AL, Koombhongse S, Reneker DH. J Appl Phys 2001;90:4836.
[9] Shin YM, Hohman MM, Brenner MP, Rutledge GC. Appl Phys Lett 2001;78:1149.
[10] Hohman MM, Shin M, Rutledge G, Brenner MP. Phys Fluids 2001;13:2201.
[11] Hohman MM, Shin M, Rutledge G, Brenner MP. Phys Fluids 2001;13:2221.
[12] Fridrikh SV, Yu JH, Brenner MP, Rutledge GC. Phys Rev Lett 2003;90:144502.
[13] Wang M, Hsieh AJ, Rutledge GC. Polymer 2005;46:3407.
[14] Li D, Wang Y, Xia Y. Nano Lett 2003;3:1167.
[15] Wang X, Kim Y, Drew C, Ku B, Kumar J, Samuelson LA. Nano Lett 2004;4:331.
[16] Jin H-J, Chen J, Karageorgious V, Altman GH, Kaplan DL. Biomaterials 2004;25:1039.
[17] Pinto NJ, Johnson Jr AT, MacDiarmid AG, Mueller CH, Theofylaktos N, Robinson DC, et al. Appl Phys Lett 2003;83:4244.
[18] Gibson PW, Schreuder-Gibson H, Rivin D. AIChE J 1999;45:190.
[19] Gibson P, Schreuder-Gibson H, Rivin D. Colloids Surf A 2001;187–188:469.
[20] Schreuder-Gibson H, Gibson P, Senecal K, Sennett M, Walker J, Yeomans W, et al. J Adv Mater 2002;34:44.
[21] Couderc S, Toullec J. Langmuir 2001;17:3819.
[22] Kassa J. J Toxicol Clin Toxicol 2002;40:803.
[23] Epstein J, Kaminski JJ, Bodor N, Enever R, Sowa J, Higuchi T. J Org Chem 1978;43:2816.
[24] Bunton CA, Ihara Y. J Org Chem 1977;42:2865.
[25] Simanenko YS, Karpichev EA, Prokop'eva TM, Panchenko BV, Bunton CA. Langmuir 2001;17:581.

[26] Kunitake T, Okahata Y. Macromolecules 1976;9:15.
[27] Kunitake T, Okahata Y, Sakamoto T. J Am Chem Soc 1976;98:7799.
[28] Bromberg L, Hatton TA. Ind Eng Chem Res 2005;44:7991.
[29] Tsang JS, Neverov AA, Brown RS. J Am Chem Soc 2003;125:7602.
[30] Miller PD, Spivey HO, Copeland SL, Sanders R, Woodruff A, Gearhart D, et al. Langmuir 2000;16:108.
[31] Schouteden FLM. Makromol Chem 1957;24:25.
[32] Shin YM, Hohman MM, Brenner MP, Rutledge GC. Polymer 2001;42:9955.
[33] Buncel E, Cannes C, Chatrousse A-P, Terrier F. J Am Chem Soc 2002;124:8766.
[34] Fornasier R, Tonellato U. J Chem Soc Faraday Trans 1 1980;76:1301.
[35] Mancin F, Tecilla P, Tonellato U. Langmuir 2000;16:227.
[36] Fanti M, Mancin F, Tecilla P, Tonellato U. Langmuir 2000;16:10115.
[37] Kunitake T, Okahata Y. Bioorg Chem 1975;4:136.
[38] Bender ML, Marshall TH. J Am Chem Soc 1968;90:201.
[39] Carey FA. In: Organic chemistry. 4th ed. Boston: McGraw Hill; 2000. p. 944.
[40] Tomoi M, Ford WT. J Am Chem Soc 1980;102:7141.
[41] Ghosh KK, Satnami ML, Sinha D, Vaidya J. J Mol Liq 2005;116:55.
[42] Soane DS, Offord DA, Linford MR, Millward DB, Ware W, Erskine L, et al. U.S. Patent 6,607,994; 2003.